

Criteria for the accuracy of small polaron quantum master equation in simulating excitation energy transfer dynamics

Hung-Tzu Chang, Pan-Pan Zhang, and Yuan-Chung Cheng

Citation: *The Journal of Chemical Physics* **139**, 224112 (2013); doi: 10.1063/1.4840795

View online: <http://dx.doi.org/10.1063/1.4840795>

View Table of Contents: <http://scitation.aip.org/content/aip/journal/jcp/139/22?ver=pdfcov>

Published by the [AIP Publishing](#)



Re-register for Table of Content Alerts

Create a profile.



Sign up today!



Criteria for the accuracy of small polaron quantum master equation in simulating excitation energy transfer dynamics

Hung-Tzu Chang,¹ Pan-Pan Zhang,² and Yuan-Chung Cheng^{1,a)}

¹Department of Chemistry and Center for Quantum Science and Engineering, National Taiwan University, Taipei City 106, Taiwan

²Department of Physics and Institute of Modern Physics, Ningbo University, Ningbo 315211, China

(Received 20 September 2013; accepted 22 November 2013; published online 13 December 2013)

The small polaron quantum master equation (SPQME) proposed by Jang *et al.* [J. Chem. Phys. **129**, 101104 (2008)] is a promising approach to describe coherent excitation energy transfer dynamics in complex molecular systems. To determine the applicable regime of the SPQME approach, we perform a comprehensive investigation of its accuracy by comparing its simulated population dynamics with numerically exact quasi-adiabatic path integral calculations. We demonstrate that the SPQME method yields accurate dynamics in a wide parameter range. Furthermore, our results show that the accuracy of polaron theory depends strongly upon the degree of exciton delocalization and timescale of polaron formation. Finally, we propose a simple criterion to assess the applicability of the SPQME theory that ensures the reliability of practical simulations of energy transfer dynamics with SPQME in light-harvesting systems. © 2013 AIP Publishing LLC. [<http://dx.doi.org/10.1063/1.4840795>]

I. INTRODUCTION

Excitation energy transfer (EET) is ubiquitous in light harvesting systems: in photosynthetic complexes of plants and algae, energy of solar irradiation is collected through electronic excitation of chlorophylls and transferred to the reaction center to drive subsequent chemical reactions;¹ in organic photovoltaics, photo-excitations of organic molecules migrate through their supporting substrates and after reaching junction interfaces, generate charges that can be collected at the electrodes to supply electricity.² One major challenge for theoretical modelling of such processes is the correct assessment of the influence from surrounding environments on electronic excitations. When the system-environment coupling is far stronger than the coupling between excited states of each single chromophores, termed as “electronic coupling,” Förster-Dexter theory is an appropriate method to describe EET. For the opposite limit where system-environment coupling is weak, Redfield theory serves as an accurate tool to simulate EET.^{3–6}

Despite their simplicity in computation and clarity in the elucidation of photophysical phenomena, recent spectroscopic experiments on photosynthetic complexes and organic materials have indicated that the adequacy of using Redfield or Förster-Dexter theories to describe EET in such systems could be questionable.^{7–12} To remedy their deficiencies, various numerically exact non-perturbative approaches have been proposed and successfully implemented to investigate EET in photosynthetic complexes.^{13–20} Though these non-perturbative methods have a clear advantage in their accuracy, the perturbative approaches still retain particular importance and usefulness in computational efficiency and direct conveyance of physical intuitions. To go beyond the

limit of Redfield and Förster theory, Jang *et al.*,^{21–23} and independently Nazir and co-workers,^{24–26} have developed a second-order, time-local, non-Markovian small polaron quantum master equation (SPQME) for coherent energy transfer in molecular systems. In addition, for specific forms of correlations between phonon excitations, Nazir and co-workers have recently developed a variational polaron master equation approach with significantly improved accuracy and range of applicability based on the theory developed by Silbey and Harris.^{27–30}

The small polaron quantum master equation is exact at the weak electronic coupling and weak system-environment coupling limits, and it can serve as a bridge between the Redfield and Förster regimes.^{31,32} SPQME has been successfully utilized to explore the role of environmental fluctuations and correlations of phonon excitations in EET dynamics.^{24,25,33} It has also been employed in the investigations of vibrational contributions to EET in photosynthetic complexes of cryptophyte algae.³⁴ However, due to its perturbative nature, the accuracy of SPQME declines in the intermediate coupling regime. For example, comparisons with variational polaron simulations show that when bath relaxation is far slower than electronic energy transfer, small polaron theory largely underestimates coherence in EET dynamics.^{28,35}

To utilize SPQME theory for accurate elucidation of physical mechanisms of EET in light harvesting systems, it is crucial to obtain a systematic assessment of its applicability throughout a wide parameter range. Recently, Cao and co-workers have investigated the equilibrium states in the small polaron theory to probe its applicable regime. Their results comply with the variational polaron studies;³⁶ however, the accuracy of equilibrium structure does not fully stipulate the corresponding properties in perturbative simulations of EET dynamics. In this work, we focus on dynamics and present a comprehensive investigation of the accuracy of SPQME in simulating EET dynamics through

^{a)}Electronic mail: yuanchung@ntu.edu.tw

comparisons with numerically exact quasi-adiabatic path integral (QUAPI) calculations.^{13,14} With this comprehensive benchmark, we shall also propose a simple criterion to determine the applicable regime of the small polaron theory.

The present work is organized as follows. In Sec. II, we will first review the formalism of SPQME and present a dimer model system for the comparison of EET dynamics simulated by small polaron master equation and QUAPI. The results of comparison will be presented in Sec. III along with discussions about the adequacy of the small polaron theory (SPQME) in various parameter regimes and its underlying physics. Finally, we shall summarize the previous comparison results with a simple criterion for the determination of the regime of applicability of the small polaron theory in Sec. IV.

II. THEORY

A. Small polaron transformation

To study EET in light harvesting systems, we consider a Frenkel exciton model Hamiltonian including the singly excited states of N chromophores coupled to a harmonic bath through bilinear system-bath couplings ($\hbar = 1$),^{37,38}

$$\begin{aligned} H &= H_s + H_b + H_{sb}, \\ H_s &= \sum_i \mathcal{E}_i a_i^\dagger a_i + \sum_{i \neq j} J_{ij} a_i^\dagger a_j, \\ H_b &= \sum_n \omega_n (b_n^\dagger b_n + 1/2), \\ H_{sb} &= \sum_{i,n} \omega_n g_{ni} a_i^\dagger a_i (b_n + b_n^\dagger), \end{aligned} \quad (1)$$

where H_s is the Hamiltonian for the electronic system with \mathcal{E}_i denoting the optical transition energy of the i th chromophore (site) and J_{ij} marking the electronic coupling between the i th and j th site; a_i^\dagger is the creation operator of excitation on the i th chromophore. H_b is the harmonic bath Hamiltonian with b_n^\dagger as the creation operator and ω_n as the frequency of the n th phonon mode. H_{sb} describes the system-bath couplings with g_{ni} denoting the electron-phonon coupling constant between the n th phonon mode and the i th site.

Excitations and charges in condensed matter will polarize their surrounding vibrations and hence while considering exciton and charge transport problems in a condensed matter, it is often appropriate to envisage such phenomena from a representation that combines the excitation with its surrounding polarization as an entity, a “polaron,” rather than considering the exciton and polarized bath separately. The transformation from a bare-excitonic to a polaronic perspective can be accomplished by the small polaron transformation, whose formalism was pioneered by Holstein and later used by Silbey and co-workers to study charge transport properties of organic molecular crystals.^{31,39} The small polaron transformation operator, which displaces the origin of the bath coordinates to the excited-state vibrational equilibrium, can be expressed as $U = e^S$, with $S = \sum_{i,n} g_{ni} a_i^\dagger a_i (b_n - b_n^\dagger)$. Applying small polaron transformation to the bare exciton Hamiltonian effectively converts the system to a “polaron” basis to yield the

polaron Hamiltonian,

$$\begin{aligned} \tilde{H} &= U^\dagger H U = \tilde{H}_s + \tilde{H}_{sb} + \tilde{H}_b, \\ \tilde{H}_s &= \sum_i (\mathcal{E}_i - \lambda_i) a_i^\dagger a_i + \sum_{i \neq j} J_{ij} \langle \theta_i^\dagger \theta_j \rangle a_i^\dagger a_j, \\ \tilde{H}_b &= H_b, \\ \tilde{H}_{sb} &= \sum_{i \neq j} J_{ij} (\theta_i^\dagger \theta_j - \langle \theta_i^\dagger \theta_j \rangle), \end{aligned} \quad (2)$$

where reorganization energy of each site $\lambda_i = \sum_n g_{ni}^2 \omega_n$ is added to the site energies. During polaron transformation, the electronic couplings J_{ij} is dressed by displacement operators $\theta_i^\dagger \theta_j = e^{-\sum_n g_{ni} (b_n - b_n^\dagger)} e^{\sum_n g_{nj} (b_n - b_n^\dagger)}$. To retain coherence effects in the zeroth order Hamiltonian, the dressed electronic coupling term $J_{ij} \theta_i^\dagger \theta_j$ is deliberately separated into its environmental thermal average $J_{ij} \langle \theta_i^\dagger \theta_j \rangle$ and fluctuations $J_{ij} (\theta_i^\dagger \theta_j - \langle \theta_i^\dagger \theta_j \rangle)$, with the former added back to the system Hamiltonian and the latter taken as the new system-bath coupling term. As a result, the electronic coupling J_{ij} is endowed with a renormalization factor $\langle \theta_i^\dagger \theta_j \rangle$, which is a Frank-Condon factor describing the overlap of the phonon wavefunctions between the polaronic state on site i and j given by

$$\langle \theta_i^\dagger \theta_j \rangle = \exp \left[-\frac{1}{2} \sum_n (g_{ni} - g_{nj})^2 \coth \frac{\beta \omega_n}{2} \right],$$

with inverse temperature $\beta = (k_B T)^{-1}$.

The inclusion of thermally renormalized electronic couplings $J_{ij} \langle \theta_i^\dagger \theta_j \rangle$ back into the zeroth order Hamiltonian is a special feature of the small polaron theory that distinguishes it from non-interacting-blip approximation and Kenkre and Knox’s generalized master equation approaches,^{40–42} in which the full renormalized electronic couplings are taken as the perturbation. The thermal-averaged renormalized electronic coupling in the zeroth order Hamiltonian introduces temperature and electron-phonon coupling dependence to the structure of electronic equilibrium density matrix. As a result, the electronic couplings diminish to zero when temperature or electron-phonon couplings are large. This leads to the physical prediction of dynamical localization that the electronic eigenstates are localized at high temperature and strong electron-phonon couplings.^{33,43}

The renormalized system-bath coupling, \tilde{H}_{sb} , describes the fluctuations of phonon-dressed electronic couplings. This term is intentionally chosen so that it goes to zero at both the weak electronic coupling and weak electron-phonon coupling limits, i.e., when either J or g goes to zero.⁴⁴ Thus, the Hamiltonian can be exactly solved at both the weak electronic coupling and weak electron-phonon coupling limits.

B. Small polaron quantum master equation

The small polaron theory has long been utilized to study exciton migration and charge transport properties in solids, yet previous studies have been focusing on diagonal population transfer.^{27,31,32,39} However, recent spectroscopic experiments suggest that quantum coherence plays an important role in EET of photosynthetic complexes as well as organic

semiconductors.^{8,9} Motivated by these new empirical discoveries, Jang *et al.* generalized the small polaron formalism to incorporate off-diagonal dynamics.^{6,21}

Following Zwanzig's projection operator formalism, a small polaron quantum master equation (SPQME) of the reduced density matrix in the polaron representation can be derived,²³

$$\begin{aligned} \dot{\sigma}(t) = & -i[\tilde{H}_s, \sigma(t)] - \int_0^t d\tau \text{Tr}_b \\ & \{ [\tilde{H}_{sb}(0), [\tilde{H}_{sb}(-\tau), \sigma(t) \otimes \rho_b^{eq}]] \} \\ & - i \text{Tr}_b \{ [\tilde{H}_{sb}(0), e^{-i(\tilde{H}_s + \tilde{H}_b)t} \\ & \times (\rho_T(0) - \sigma(0) \otimes \rho_b^{eq}) e^{i(\tilde{H}_s + \tilde{H}_b)t}] \} \\ & - \int_0^t d\tau \text{Tr}_b \{ [\tilde{H}_{sb}(0), [\tilde{H}_{sb}(\tau - t), e^{-i(\tilde{H}_s + \tilde{H}_b)t} \\ & \times (\rho_T(0) - \sigma(0) \otimes \rho_b^{eq}) e^{i(\tilde{H}_s + \tilde{H}_b)t}] \} \}, \quad (3) \end{aligned}$$

where $\text{Tr}_b\{\}$ denotes trace over bath degrees of freedom and ρ_b^{eq} is the bath equilibrium density matrix of H_b . The time evolution of an operator $A(\tau)$ is defined in the interaction picture of the zeroth Hamiltonian, $\tilde{H}_0 = \tilde{H}_s + \tilde{H}_b$.

The first term in the polaron master equation (Eq. (3)) describes coherent dynamics. The second term accounts for the dissipative dynamics induced by system-bath couplings. The last two terms are the inhomogeneous terms which incorporate contributions from non-equilibrium bath dynamics to EET and go to zero after bath reaches thermal equilibrium.²¹ The inhomogeneous terms in SPQME (Eq. (3)) contain three-time bath correlation functions which entail significant computational resources in EET simulation. By assuming fast bath relaxation, the inhomogeneous terms can be omitted to yield

$$\begin{aligned} \dot{\sigma}(t) = & -i[\tilde{H}_s, \sigma(t)] \\ & - \int_0^t d\tau \text{Tr}_b \{ [\tilde{H}_{sb}(0), [\tilde{H}_{sb}(-\tau), \sigma(t) \otimes \rho_b^{eq}]] \}. \quad (4) \end{aligned}$$

In Sec. III, we investigate the accuracy of EET simulations obtained from both master equations with and without inhomogeneous terms (Eqs. (3) and (4), respectively) by comparing the computational results from SPQME with numerically exact QUAPI calculations. Since SPQME is expected to bridge between conventional Redfield and Förster theories, we focus on EET dynamics in the intermediate regime where electronic couplings and reorganization energies are comparable.

C. Dimer model system

The small polaron quantum master equation (Eq. (3)) is general and valid for multichromophoric systems. Yet to illustrate the physical picture for the regime of applicability of the master equation, we confine ourselves to a simple model system with a donor and an acceptor. We define the untrans-

formed system Hamiltonian of the dimer as

$$H_s = \begin{pmatrix} \Delta & J \\ J & -\Delta \end{pmatrix},$$

where 2Δ is the energy gap, and J is the bare electronic coupling before polaron transformation.

To treat system-bath couplings, we introduce spectral-density

$$\tilde{\gamma}_{ij}(\omega) = \sum_n g_{ni} g_{nj} \omega_n^2 \delta(\omega - \omega_n) = \gamma_{ij} \mathfrak{K}(\omega), \quad (5)$$

where γ is a unit-less electron-phonon coupling constant: γ_{ii} measures the electron-phonon coupling strength on the i th site and γ_{ij} ($i \neq j$) describes the electron-phonon coupling strength shared between the i th and j th chromophore. In this article, we consider a super-Ohmic spectral density to treat the system-bath couplings,

$$\mathfrak{K}(\omega) = \frac{\omega^3}{\omega_c^2} e^{-\frac{\omega}{\omega_c}}, \quad (6)$$

where ω_c is the cut-off frequency, which we take as the unit of energy in this work ($\omega_c = 1$). Note that for Ohmic and sub-Ohmic spectral densities, the renormalized electronic couplings will always be zero regardless of electron-phonon coupling strength due to divergence of integral in the Frank-Condon factor $\langle \theta_i^\dagger \theta_j \rangle$. Thus, for these over-damped baths, the small polaron theory can only describe incoherent dynamics.²⁸ For simplicity, we consider the bath of the donor and acceptor to be identical and independent throughout this article, i.e., $\gamma_{ij} = \gamma \delta_{ij}$.

D. QUAPI simulations

The accuracy of SPQME is investigated by comparing its simulated site population dynamics with numerically exact QUAPI simulations, for which we follow the methods prescribed by Makri and Makarov.¹³ For simplicity, we assume that the initial density matrix is the Frank-Condon excitation on site 1 and the interaction between system and bath is switched on at zero time ($t = 0$),

$$\rho(0) = \rho_s(0) \otimes \rho_{bath}(0) = \begin{pmatrix} 1 & 0 \\ 0 & 0 \end{pmatrix} \otimes \rho_{b,g}^{eq},$$

where $\rho_{b,g}^{eq}$ denotes the equilibrium bath density matrix of electronic ground state.

With the above initial condition, the time evolution of the reduced density matrix of the excitonic system is given by

$$\begin{aligned} \rho_s(s'', s'; t) = & \text{Tr}_b \langle s'' | e^{-iHt/\hbar} \rho(0) e^{iHt/\hbar} | s' \rangle \\ = & \int ds_0^+ \int ds_1^+ \cdots \int ds_{N-1}^+ \int ds_0^- \\ & \times \int ds_0^- \cdots \int ds_{N-1}^- \\ & \times \langle s'' | e^{-iH_s \Delta t/\hbar} | s_{N-1}^+ \rangle \cdots \langle s_1^+ | e^{-iH_s \Delta t/\hbar} | s_0^+ \rangle \\ & \times \langle s_0^+ | \rho_s(0) | s_0^- \rangle \langle s_0^- | e^{iH_s \Delta t/\hbar} | s_1^- \rangle \cdots \end{aligned}$$

$$\begin{aligned} & \times \langle s_{N-1}^- | e^{iH_s \Delta t / \hbar} | s' \rangle \\ & \times I(s_0^+, s_1^+, \dots, s_{N-1}^+, s'', s_0^-, \dots, s_{N-1}^-, s'; \Delta t), \end{aligned} \quad (7)$$

where the influence functional I takes the form^{13,45}

$$I = \exp \left\{ -\frac{1}{\hbar} \sum_{k=0}^N \sum_{k'=0}^k (s_k^+ - s_k^-) (\eta_{kk'} s_{k'}^+ - \eta_{kk'}^* s_{k'}^-) \right\},$$

and the definitions of parameters $\eta_{kk'}$, $\eta_{kk'}^*$ can be found in Ref. 13.

For the numerical scheme of QUAPI, we follow the method detailed in Refs. 14 and 46. Here we should briefly recount their approach in reaching numerical convergence. The propagation of density matrix is exact in Eq. (7) at the limit $\Delta t \rightarrow 0$. With finite time slice Δt in practical calculation, numerical convergence should be found by reducing Δt to a small enough value. On the other hand, to handle the bath correlations in the influence functional, a memory-time window $\tau_m = N\Delta t$ has to be created in which the bath correlations are exactly computed. To reach converged results, the memory-time window should be enlarged by increasing N such that all bath correlations are included. In our calculations, we vary the value N and Δt for each parameter set individually using this procedure to ensure convergence in all numerical calculations.

III. RESULTS AND DISCUSSIONS

A. Convergence of perturbation expansion

Before we present the comparison between SPQME and QUAPI, we discuss the previously proposed criteria for the accuracy of small polaron methods to guide our evaluation of the applicable regime of SPQME. The accuracy of a perturbative approach should depend upon the magnitude of the perturbative term. For the polaron master equation, Jang has estimated the magnitude of perturbation through the variance of the perturbative term \tilde{H}_{sb} .²² In a similar fashion, while investigating the Rabi oscillations of a single quantum dot system, McCutcheon and Nazir have proposed an estimation for the applicable regime of their Markovian polaron master equation by considering the magnitude of the fourth-order perturbation term.⁴⁷ When the thermal average of perturbative terms are small, the perturbative approach should yield accurate results. Here we will review their considerations and in Secs. III B–III E extend their results to obtain the criteria for the applicability of the small polaron theory.

Following Jang's work, we first examine the variance of the perturbative term

$$\text{Tr}_b \{ \tilde{H}_{sb}^2 \rho_b^{eq} \} = J^2 (1 - \langle \theta_1^\dagger \theta_2 \rangle^2) \mathbb{I}_s, \quad (8)$$

where \mathbb{I}_s is the identity operator of the electronic part and $\langle \theta_1^\dagger \theta_2 \rangle$ is the Frank-Condon factor for the polaronic excited states of site 1 and 2. Equation (8) indicates that we can define a unit-less parameter κ to quantify the magnitude of the perturbation,

$$\kappa = (J/\omega_c) \sqrt{1 - \langle \theta_1^\dagger \theta_2 \rangle^2}. \quad (9)$$

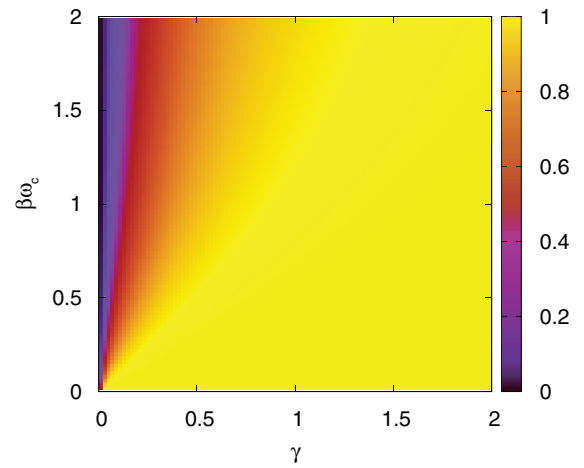


FIG. 1. Electron-phonon contribution to the magnitude of perturbation parameter, $1 - \langle \theta_1^\dagger \theta_2 \rangle^2$, as a function of γ and $\beta\omega_c$. Here we show that the electron-phonon contribution approaches zero only in extremely weak electron-phonon couplings.

It should be noted that although the choice of energy unit that makes κ unit-less may seem to be arbitrary, the introduction of cut-off frequency ω_c into κ furnishes this parameter with the physical consideration of the time scale of polaron formation, which shall be further discussed in Sec. III B. In this dimer model, the electronic and electron-phonon coupling dependences in κ are separated. For the electronic part, κ is proportional to J , whereas electron-phonon couplings contribute to the term $\sqrt{1 - \langle \theta_1^\dagger \theta_2 \rangle^2}$ that is always less than 1. The Frank-Condon factor $\langle \theta_1^\dagger \theta_2 \rangle$ depends exponentially upon electron-phonon coupling strength γ ,

$$\begin{aligned} \langle \theta_1^\dagger \theta_2 \rangle &= \exp \left[-\frac{1}{2} \sum_n (g_{n1} - g_{n2})^2 \coth \frac{\beta\omega_n}{2} \right] \\ &= \exp \left[-\gamma \int_0^\infty \frac{\mathfrak{R}(\omega)}{\omega^2} \coth \frac{\beta\omega}{2} d\omega \right]. \end{aligned}$$

The small polaron approach should be valid when $\kappa \ll 1$.

The electron-phonon contribution to the magnitude of perturbation, $1 - \langle \theta_1^\dagger \theta_2 \rangle^2$, for the dimer model is plotted in Fig. 1 as a function of the electron-phonon coupling strength γ and inverse temperature β . In intermediate and strong electron-phonon coupling regimes, the electron-phonon contribution approaches 1 and it only decreases to zero at extremely weak electron-phonon couplings. Figure 1 shows that the value of $1 - \langle \theta_1^\dagger \theta_2 \rangle^2$ is close to unity across a broad parameter regime, and thus the magnitude of parameter κ is dominated by J . Hence, according to this criterion, SPQME should yield accurate results when $J/\omega_c < 1$ or when electron-phonon coupling is extremely weak. Furthermore, noticing that $1 - \langle \theta_1^\dagger \theta_2 \rangle^2$ is not sensitive to γ and temperature in the parameter regime studied in this work (Fig. 1), we conclude that κ alone does not provide a sensitive criterion for the applicability of the SPQME method.

To probe the convergence of the perturbation series, one can also compare the magnitude of the second order

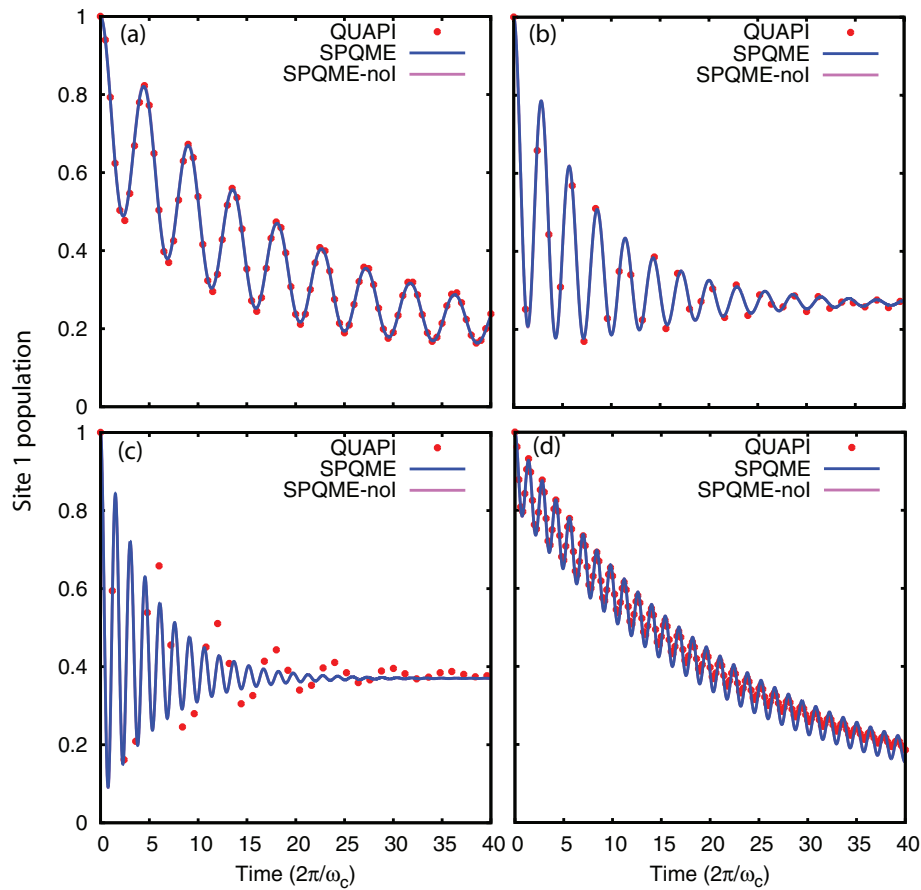


FIG. 2. Comparison of population dynamics simulated by SPQME and QUAPI in weak electron-phonon coupling regime ($\gamma = 0.2/\pi$ and $k_B T = 0.5\omega_c$). The EET dynamics simulated by full SPQME (Eq. (3)) is denoted by “SPQME” in legend and the master equation without inhomogeneous terms (Eq. (4)) is denoted by “SPQME-noI”. In (a)–(c), Δ is set to $0.5\omega_c$ and each with $J\omega_c = 0.5, 1$, and 2 . In (d), we calculate with $\Delta = 2\omega_c$ and $J\omega_c = 1$ to probe the influence of energy gap on the accuracy of SPQME simulation.

perturbation term with that of the next order term.⁴⁷ Since the third order term is zero because $\langle \tilde{H}_{sb} \rangle_b = 0$, we calculate the fourth order perturbation $\langle \tilde{H}_{sb}^4 \rangle_b$,

$$\langle \tilde{H}_{sb}^4 \rangle_b = J^4 (1 - \langle \theta_1^\dagger \theta_2 \rangle^4) \mathbb{I}_s.$$

The electron-phonon contribution $1 - \langle \theta_1^\dagger \theta_2 \rangle^4$ approaches unity more rapidly than its second-order counterpart due to faster decay contributed by the exponent on Frank-Condon factor, and therefore the value of J determines the magnitude of the fourth order perturbation term. From the preceding analyses, the convergence behaviour deduced from second and fourth order perturbation terms is the same, because the magnitudes of both terms are dominated by electronic coupling J . Regarding the electron-phonon coupling contribution, the magnitude of perturbative term only reaches a small value at the weak electron-phonon coupling limit. In addition, the magnitude of perturbation at a fixed J value is raised to maximum at strong electron-phonon coupling limit. This contradicts the conventional wisdom that the polaron basis should become the optimal representation for the excited states and the small polaron approach should become exact at the strong electron-phonon coupling limit.^{27,28,35,36} We shall further investigate this point in Sec. III C.

B. Bath relaxation and coherence

Aside from the magnitude of perturbation, the timescales of bath relaxation and resonant energy transfer also have significant impact on the accuracy of the polaron approach.^{28,36,47} In the polaron representation, the exciton is always accompanied by its induced bath polarization, which suggests that the polaron approach is applicable when the rate of the induction of bath polarization is faster than, or similar to, the changes of population on a single chromophore. When bath relaxation is slower than changes in site population, the polaronic states do not form an appropriate basis for simulations of EET dynamics.^{28,35,36}

In general, the transfer of site population can be characterized by an oscillating coherent part and an exponential population decay in the Markovian limit. When coherent dynamics dominates, the site population oscillates with a frequency determined by the exciton energy gap (Figs. 2(a)–2(c)), which is given by $2\sqrt{\Delta^2 + J^2}$ in the dimer model. Furthermore, the bath relaxation time is inversely proportional to the cut-off frequency ω_c .^{47,48}

To examine the applicability of the SPQME method, we have performed a comprehensive benchmark of the SPQME theory against the QUAPI approach. A few representative examples are shown in Fig. 2. In Figs. 2(a)–2(c), we compare SPQME with numerically exact QUAPI calculations for a

dimer with three different electronic couplings in the coherent regime ($\gamma = 0.2/\pi$), with site energy gap $2\Delta = \omega_c$. In this comparison, SPQME performs extremely well in a broad parameter regime: at the fast bath limit (Fig. 2(a), $J/\omega_c = 0.5$), EET dynamics obtained from the small polaron theory and QUAPI agree excellently; as the exciton energy gap becomes larger and comparable to the bath cut-off frequency (Fig. 2(b), $J/\omega_c = 1$), SPQME still reproduces the exact results. However, SPQME underestimates the amplitude of coherent oscillations and the timescale of decoherence when exciton energy gap far exceeds the bath cut-off frequency (Fig. 2(c), $J/\omega_c = 2$). In this regime, the bath relaxes much slower than the coherent EET dynamics. Whereas the small polaron theory enforces a full displacement of bath coordinates to excited state vibrational equilibrium, the slow bath relaxation renders the “undisplaced,” or “partially displaced” representations more appropriate for the description of dynamics. Choosing the small polaron representation, or full displacement of bath coordinates in the slow bath regime over-dresses the electronic couplings, which results in the underestimation of exciton delocalization and coherence that has already been shown in variational polaron studies.^{28,30,35,36}

The performance of small polaron theory under various electronic couplings shows that the magnitude between exciton energy gap and bath cut-off frequency provides an indicator of the accuracy for SPQME in the coherent regime. With such physical picture in mind, we arrive at a criterion for the applicable regime of the small polaron theory

$$\psi = \sqrt{\Delta^2 + J^2}/\omega_c < 1. \quad (10)$$

When the electronic parameters satisfy such inequality, SPQME should yield excellent results. In addition, because energy gap should be small compared to electronic coupling in the coherent regime, we can omit Δ in the above expression and obtain a simpler form,

$$\psi' = J/\omega_c < 1. \quad (11)$$

This simplified expression coincides with the estimation deduced from the magnitude of perturbation ($\kappa \sim J/\omega_c \ll 1$) as discussed in Sec. III A.

Through the previous comparisons we demonstrate that the performance of SPQME depends strongly upon the ratio between bath cut-off frequency and exciton energy gap when coherent EET dynamics dominates. However, as exciton transfer becomes incoherent due to the increase of site energy gap or electron-phonon couplings, the timescale of EET dynamics cannot be characterized solely by the exciton energy gap that determines coherent oscillation frequency. As a result, the relationship between bath cut-off frequency and exciton energy gap no longer serves as a suitable indicator for the performance of SPQME. In our benchmarks, we found that for an incoherent system that exhibits exciton energy gap much larger than bath cut-off frequency, SPQME may produce accurate results. In Fig. 2(d), we show the simulated dynamics with large site energy gap ($\Delta = 2\omega_c$ and $J/\omega_c = 1$). The coherent oscillation in Fig. 2(d) is suppressed by the large site energy gap and the exponential population decay becomes prominent. Figure 2(d) shows that when EET becomes incoherent, small polaron theory still provides accurate dynamics

even though the exciton energy gap exceeds the bath cut-off frequency.

In a more extensive comparison (data not shown), we found that such improvement of accuracy for large site energy gap ($\Delta/J > 1$) is universal when the dynamics is overly-damped. As energy transfer becomes incoherent, the applicable regime of small polaron theory spans well out of the bound estimated by criteria ψ and ψ' (Eqs. (10) and (11)), since the strongly oscillatory dynamics in coherent regime is reduced to slow population decay. The change of behaviour in population transfer from fast oscillation to slow exponential decay allows longer timescale for polaron formation, which extends the applicable regime of the small polaron theory. The transition to incoherent regime can be achieved by the increase of energy gap, temperature, or electron-phonon coupling strength. In Secs. III C–III D, we shall explore the other factors that controls the coherence of the system: the electron-phonon coupling strength and temperature.

C. Electron-phonon couplings

The performance of the small polaron theory strongly depends on the strength of electron-phonon couplings, which has been the subject of many studies.^{28,35,36} In Sec. III B, we have investigated the validity of SPQME in the weak electron-phonon coupling regime (Fig. 2). In the strong electron-phonon coupling regime, excitations are accompanied by strong distortion of surrounding vibrations, rendering the small polaron picture an appropriate representation to describe EET dynamics.^{27,28,35,36} However, the performance of SPQME in the intermediate coupling regime has not been fully explored. In this section, we investigate the applicability of SPQME across the whole range of electron-phonon couplings and present a few representative examples.

In our benchmark against QUAPI, we found that at the fast bath limit ($\psi' < 1$), SPQME provides reasonable results regardless of electron-phonon parameters. Figure 3 demonstrates that small polaron theory can bridge between the weak and strong electron-phonon coupling limits: from weak (Fig. 3(a), $\gamma = 0.2/\pi$) to strong (Fig. 3(c), $\gamma = 2/\pi$) electron-phonon couplings, population dynamics simulated by SPQME corresponds nicely with QUAPI results. Though SPQME does not reproduce the exact short-time dynamics in the intermediate electron-phonon coupling regime (Fig. 3(b)), it still yields accurate decoherence time and population relaxation time. Note that the inhomogeneous term contribution affects the early-time dynamics in this case, implicating that the bath memory effects neglected by the time-local SPQME approach could explain the discrepancy in the short-time dynamics.

In contrast, when electronic coupling is strong, i.e., slow bath ($\psi' > 1$), the accuracy of the SPQME approach declines. Figure 4 displays the dynamics in the slow bath regime ($\psi' = J/\omega_c = 2$) with various electron-phonon coupling strengths. At weak electron-phonon coupling (Fig. 4(a)), coherent dynamics is dominant and SPQME significantly underestimates the decoherence time and the amplitude of coherent oscillations. However, when electron-phonon couplings

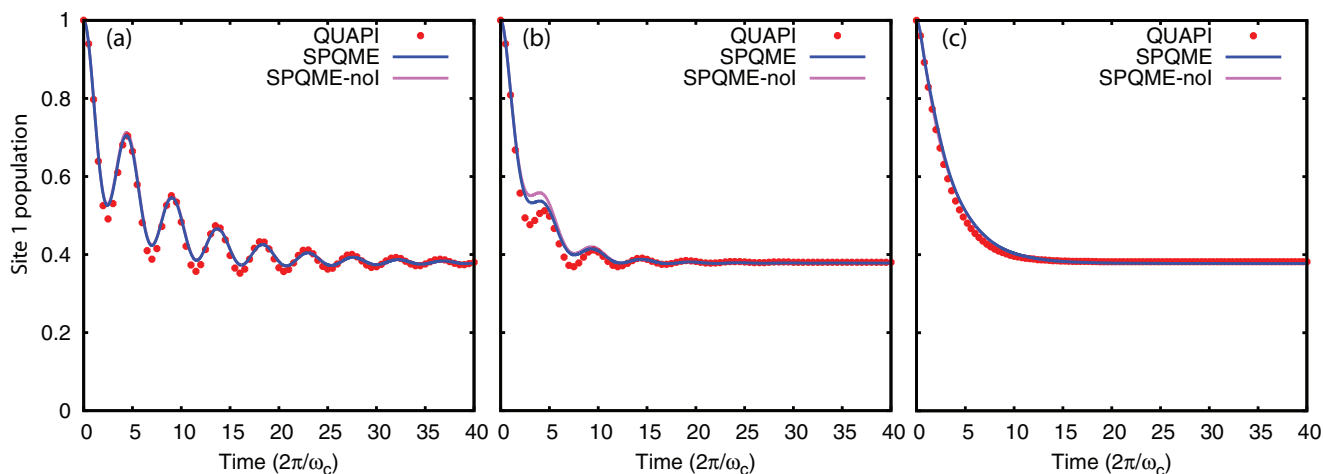


FIG. 3. Comparison of population dynamics simulated by SPQME and QUAPI at weak electronic coupling ($J = 0.5\omega_c$) with different electron-phonon coupling strengths: (a) $\gamma = 0.2/\pi$; (b) $\gamma = 0.5/\pi$; and (c) $\gamma = 2/\pi$. Other parameters are set as $\Delta = 0.5\omega_c$ and $k_B T = 2\omega_c$.

are strong, the applicable range of the small polaron theory expands into the slow bath region (Fig. 4(c)). The increase of electron-phonon couplings suppresses coherence, making the site-localized basis a suitable representation for describing energy transfer dynamics. Therefore, the small polaron theory is suitable for describing the incoherent population decay at the strong electron-phonon coupling limit.

The performance of SPQME at the weak electron-phonon coupling limit can be characterized by the parameter κ , which includes the estimation of applicability of SPQME through electronic parameter ψ' (Eq. (11)). κ approaches zero as electron-phonon coupling strength reduces to zero, where the small polaron theory is exact. However, κ cannot describe the extension of applicability of the small polaron theory to the strong electron-phonon coupling limit, where SPQME still yields accurate results (Fig. 4(c)) even if $\kappa > 1$. The failure of identifying the applicability of SPQME with κ at strong electron-phonon coupling limit can be understood by the localization of exciton states and introduction of reorganization energy. At such limit, dynamical localization dominates EET dynamics which is manifested by the renormaliza-

tion of electronic couplings in the small polaron theory.³³ As the exciton states are localized by strong phonon scattering, the site-localized basis becomes an appropriate framework to describe EET. Furthermore, as reorganization energies dominate the Hamiltonian, taking electronic coupling J as perturbation becomes adequate, which leads to Kenkre and Knox's generalized master equation approach and Förster theory.⁴² As shown by Kenkre, that the small polaron theory and the generalized master equation approach are exactly equivalent at strong electron-phonon coupling limit,⁴⁹ the applicability of SPQME in such regime is justified. From these discussions, we demonstrate that the localization of exciton states is also an important factor affecting the performance of the small polaron theory. To incorporate such effect, we should seek a more general criterion for the applicability of SPQME, which will be introduced in Sec. III E.

D. Temperature effects

The dependence of the accuracy of SPQME upon temperature is similar to its counterpart on electron-phonon

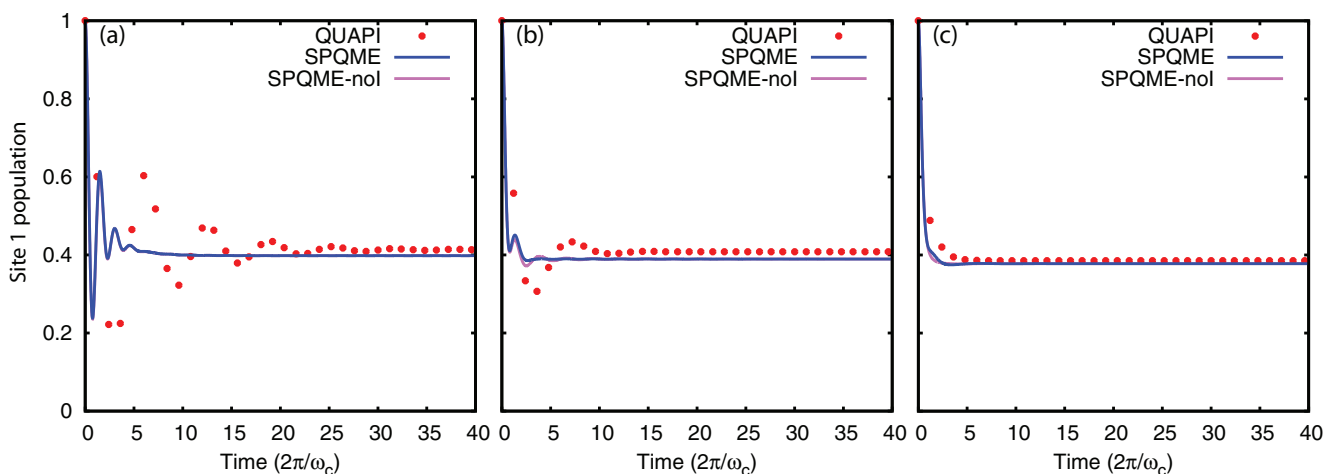


FIG. 4. Comparison of population dynamics simulated by SPQME and QUAPI at strong electronic coupling ($J = 2\omega_c$) with different electron-phonon coupling strengths: (a) $\gamma = 0.2/\pi$; (b) $\gamma = 0.5/\pi$; and (c) $\gamma = 2/\pi$. Other parameters are set as $\Delta = 0.5\omega_c$ and $k_B T = 2\omega_c$.

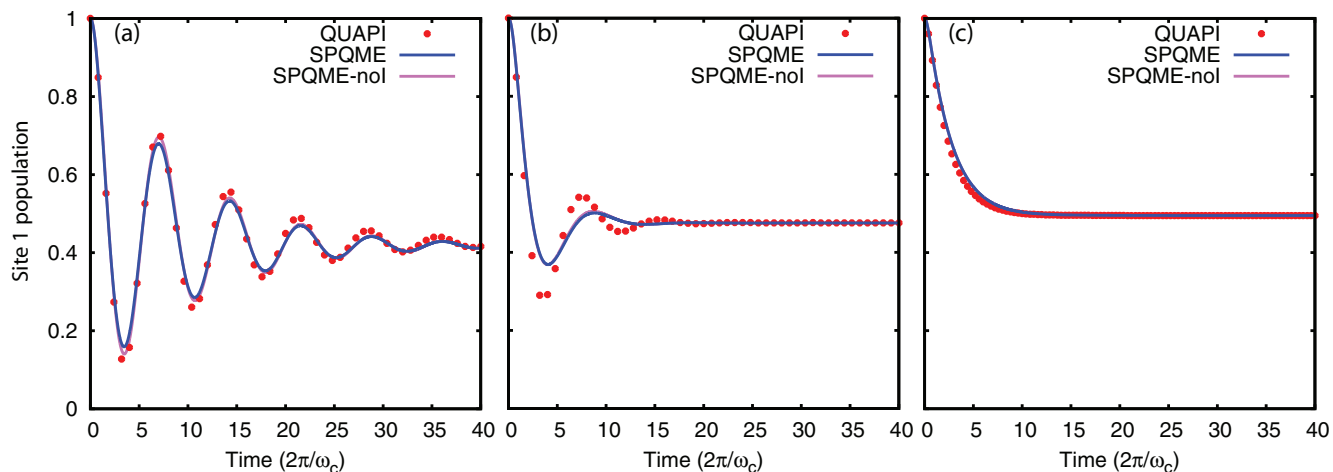


FIG. 5. Comparison of population dynamics simulated by SPQME and QUAPI at intermediate coupling regime ($\Delta = 0.1\omega_c$, $J = 0.5\omega_c$, and $\gamma = 0.5/\pi$) with different temperature: (a) $k_B T = 0.5\omega_c$, (b) $k_B T = 2\omega_c$, and (c) $k_B T = 10\omega_c$.

coupling strength. At the high temperature limit, the Frank-Condon factor $\langle \theta_1^\dagger \theta_2 \rangle$ becomes zero and such behaviour is identical to the reduction of renormalized electronic coupling at strong electron-phonon coupling limit. At high temperatures, electronic excitations are strongly scattered by the thermally excited phonons and therefore the polaron representation is expected to be an excellent framework to describe EET dynamics.^{35,43} The improvement of accuracy of SPQME with increasing temperature is shown in Figs. 5(b) and 5(c). Clearly, the small polaron theory underestimates coherence in Fig. 5(b) ($k_B T = 2\omega_c$), but is able to reproduce the exact result at a higher temperature (Fig. 5(c), $k_B T = 10\omega_c$).

At low temperatures, we observe a general improvement in the accuracy of SPQME in the fast bath regime. Comparing Fig. 5(a) with Fig. 5(b) or Fig. 2(a) with Fig. 3(a), we see that SPQME performs better as the temperature decreases. This phenomenon can be understood by considering the magnitude of perturbation. Because κ is minimized as temperature goes to zero, the outcome of SPQME calculations should approach the numerically exact results with respect to the lowering temperature.

The enhancement of the accuracy of SPQME at low temperature is nevertheless limited by the electronic parameters and electron-phonon coupling strength. At low temperatures, thermal excitations of environmental phonons are inhibited and the performance of polaron master equation is controlled by electronic parameters and electron-phonon couplings. Consequently, the dynamics simulated in slow bath and coherent regime (Fig. 2(c)) gains no improvement at low temperatures.

E. Criterion for the regime of applicability

From the comprehensive comparisons of population dynamics simulated by the SPQME approach and the numerically exact QUAPI method in both the coherent and incoherent regimes, we observe two different trends: first, in the coherent regime the SPQME approach yields excellent results when the ratio between the exciton energy gap and bath cut-

off frequency, ψ or ψ' , is small. This is the fast bath condition described by Eqs. (10) and (11), and is also captured by considering the magnitude of perturbation $\kappa < 1$ (Eq. (9)). Second, in the incoherent regime SPQME generally yields accurate results. However, since $\kappa\omega_c/J$ goes to unity in the strong electron-phonon coupling regime and ψ does not contain an electron-phonon coupling contribution, we should seek another indicator to describe the accuracy of the SPQME approach in the incoherent regime.

The transition from coherent to incoherent dynamics is strongly related to the localization of excitons, which can be determined by delocalization length taken as the inverse participation ratio of the polaron states.⁵⁰ For a dimer system, the delocalization length \mathcal{L} spans from 1, where eigenstates are completely localized, to 2, the uniformly delocalized state. In the Appendix A, we give the expressions for the delocalization length \mathcal{L} of polaronic states. We take $\sqrt{\mathcal{L} - 1}$ that is confined between 0 and 1 and multiply it by the magnitude of perturbation κ to obtain an estimation ϕ for the applicability of SPQME under both the coherent and incoherent conditions:

$$\phi = \kappa \cdot \sqrt{\mathcal{L} - 1} \ll 1. \quad (12)$$

This criterion incorporates the estimation for the degree of coherence as well as the ratio between exciton energy gap and bath cut-off frequency. Equation (12) shows that ϕ is small when the exciton is localized or when the bath relaxation is fast, and therefore we expect it to describe both two trends we observed in the comprehensive comparisons of SPQME and QUAPI.

In Figs. 6(a)–6(c), we plot ϕ as a function of electronic coupling J/ω_c and electron-phonon coupling strength γ for several site energy gaps and temperatures. These diagrams present a clear assessment for the applicable regime of the SPQME approach. In addition, we label the parameters of the representative examples shown in Figs. 2 to 4 as points on the diagrams to facilitate observation of correlation between the magnitude of ϕ values and the dynamical comparisons between SPQME and QUAPI. The behaviour of ϕ completely agrees with our dynamical comparison results. As shown in Figs. 6(a)–6(c), ϕ is small when $J/\omega_c < 1$, consistent with

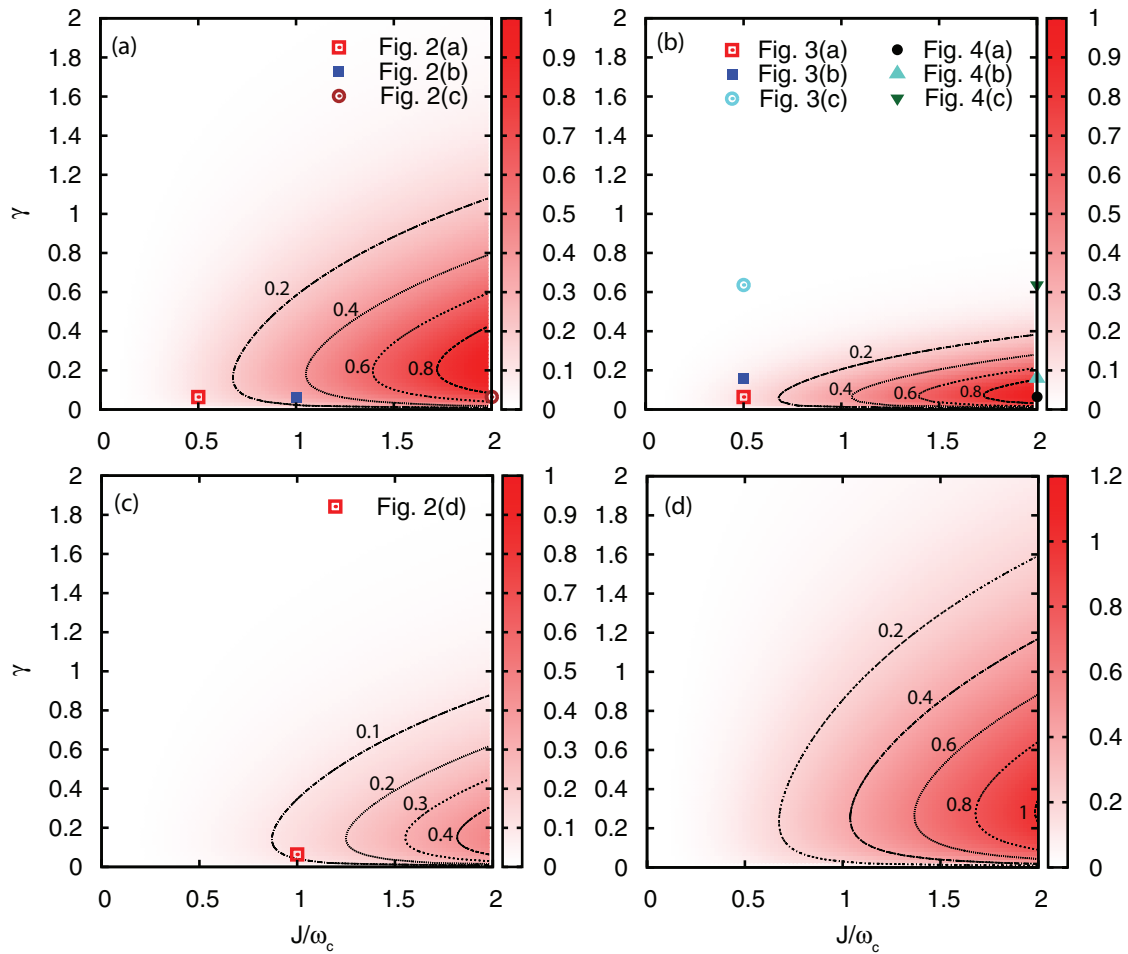


FIG. 6. Contour plots of the accuracy criteria for SPQME as a function of electronic coupling J and electron-phonon coupling strength γ . (a) ϕ at $\Delta = 0.5\omega_c$, $k_B T = 0.5\omega_c$; (b) ϕ at $\Delta = 0.5\omega_c$, $k_B T = 2\omega_c$; (c) ϕ at $\Delta = 2\omega_c$, $k_B T = 0.5\omega_c$; and (d) approximated expression ϕ' at $\Delta = 0.5\omega_c$. Additional points on (a)–(c) shows the positions on the plots for the representative cases presented in Figs. 2 to 4.

the observation that SPQME yields accurate EET dynamics under fast bath conditions. In the slow bath regime ($J/\omega_c > 1$), ϕ is large at small electron-phonon couplings and goes to zero as the electron-phonon coupling strength γ increases, reflecting that EET dynamics becomes polaronic with the increase of electron-phonon couplings. Comparing Figs. 6(a) with 6(b) and 6(c), ϕ diminishes with the increase of site energy gap Δ and temperature, in accordance with our dynamical comparisons showing that the increase of site energy gap and temperature expands the applicable regime of SPQME (Figs. 2(d) and 5). As a result, ϕ summarizes all our findings in benchmarking SPQME against QUAPI in a broad parameter regime. In general, we found that SPQME yields excellent results when $\phi < 0.5$.

Though ϕ provides an excellent criterion for the accuracy of SPQME, its value depends on the form of the spectral density and may not be easily calculated. To reach an expression that can be easily evaluated, we introduce further approximations: first, we only consider the intrinsic parameters of the system, i.e., site energy gap Δ , electronic coupling J , and electron-phonon coupling constant γ . Second, we approximate the Frank-Condon factor $\langle \theta_1^\dagger \theta_2 \rangle$ with an exponential function of γ : $\langle \theta_1^\dagger \theta_2 \rangle \sim e^{-\gamma}$, which preserves the electron-phonon contribution to exciton delocalization. With these ap-

proximations, the delocalization length factor $\sqrt{\mathcal{L} - 1}$ can be approximated as

$$\sqrt{\mathcal{L} - 1} \simeq \frac{\sqrt{2}(\sqrt{\Delta^2 + J^2 e^{-2\gamma}} - \Delta)}{|J|} \quad (13)$$

at the incoherent limit (see the Appendix A). The approximated expression yields a simple inequality for the applicable regime of SPQME that can be easily calculated:

$$\phi' = (\sqrt{\Delta^2 + J^2 e^{-2\gamma}} - \Delta)\sqrt{2 - 2e^{-2\gamma}}/\omega_c \ll 1. \quad (14)$$

In the coherent regime, the above expression reduces to the relation $J/\omega_c < 1$. In the incoherent regime, the expression goes to zero with increasing energy gap and electron-phonon couplings, or with diminished J . We plot ϕ' in Fig. 6(d). Comparing with Fig. 6(a), we show that Eq. (14) can semi-quantitatively approximate Eq. (12) at the low temperature limit.

In addition to the applicable regime of SPQME, we note that in the parameter regimes for most light-harvesting systems where both electronic couplings and reorganization energies are comparable with both frequencies, our comparisons show that the contributions of inhomogeneous terms are negligible. Though the full SPQME generally improves accuracy in short-time dynamics, the difference between the

results from Eqs. (3) and (4) is small. The insignificance of the inhomogeneous terms in our comparisons can be understood by the nature of non-equilibrium dynamics, which becomes important when bath relaxation is extremely slow or when the reorganization energy is huge so that the initial Frank-Condon excitation is far from the excited-state bath equilibrium. Since we only consider regimes of comparable electronic couplings, reorganization energies and bath frequencies, non-equilibrium effects play a minor role in the EET dynamics.

IV. CONCLUSION

In this work, we have investigated the accuracy of EET dynamics simulated by the SPQME approach through comparisons with numerically exact QUAPI results. From the comprehensive benchmark, we confirm that SPQME exhibits a wide applicable range in simulations of EET dynamics. Specifically, SPQME performs accurately in the incoherent regime where electron-phonon couplings are large and the coherent, fast bath regime where the bath relaxation is rapid. Moreover, through the particular choice of the perturbation term, the small polaron theory is also exact at the weak electron-phonon coupling limit.

With the comprehensive comparisons, we conclude that the accuracy of the small polaron theory is determined by the degree of coherence and the ratio between the exciton energy gap and bath cut-off frequency. In the incoherent regime, EET is dominated by phonon-mediated dissipation and the polaron framework becomes a natural representation to describe EET dynamics.³³ When coherent dynamics dominates, the interplay of coherent oscillation and bath relaxation (polaron formation) controls the accuracy of SPQME. When bath relaxation is faster than coherent oscillation, polaron representation is capable of describing EET dynamics accurately. When bath relaxation is slower than the electronic dynamics, the small polaron theory underrates coherence due to the overdressing in the small-polaron ansatz.^{28,35,43} Our dynamical comparisons are consistent with the investigations of equilibrium properties of the small polaron theory in Ref. 36, yet we have extended the conclusions to dynamical behaviours and revealed the importance of the coherence factor.

Incorporating these factors, we have proposed simple parameters ϕ and ϕ' to estimate the applicable regime of SPQME. We have demonstrated that ϕ and ϕ' successfully summarize the applicable regimes of the SPQME approach. We believe our investigations in this work not only provide a reliable assertion of the applicable range of the small polaron theory for its applications to EET dynamics in molecular systems, but also reveal the nature of EET dynamics in broader parameter regimes. Our results also indicate that exciton delocalization length and bath relaxation time are two key factors affecting the accuracy of the small polaron method.

As an additional note, our proposed criterion should be relevant to other polaronic theories. For example, in the development of reduced density matrix hybrid approach, Berkelbach *et al.* found a similar criterion ($J < \omega_c$) for the applicable regime of NIBA.⁵¹ Besides, they discovered that semiclassical Ehrenfest method performs well in the opposite regime

($J > \omega_c$). These findings could serve as a useful insight to guide future improvements of the small polaron theory or developments of novel theoretical methods for EET dynamics that could complement the SPQME approach.

ACKNOWLEDGMENTS

Y.C.C. thanks the National Science Council, Taiwan (Grant No. NSC 100-2113-M-002-008-MY3), National Taiwan University (Grant No. 101R891305), and Center for Quantum Science and Engineering (Subproject: 101R891401) for financial support. We are grateful to Computer and Information Networking Center, National Taiwan University for the support of high-performance computing facilities. We are also grateful to the National Center for High-Performance Computing for computer time and facilities.

APPENDIX: APPROXIMATION FOR DELOCALIZATION LENGTH

The delocalization length \mathcal{L} of an exciton state is taken as the inverse participation ratio of its exciton wave function. In the dimer model system, the delocalization length of the two electronic eigenstates are the same and can be expressed as

$$\mathcal{L} = \frac{(x^2 + y^2)^2}{x^4 + y^4}, \quad (\text{A1})$$

with $x = \sqrt{\Delta^2 + J^2\langle\theta_1^\dagger\theta_2\rangle^2} - \Delta$ and $y = J\langle\theta_1^\dagger\theta_2\rangle$. The delocalization factor $\mathcal{L} - 1$ can thus be written as

$$\mathcal{L} - 1 = \frac{2}{\left(\frac{x}{y}\right)^2 + \left(\frac{y}{x}\right)^2}.$$

Since x/y goes to zero as the dynamics becomes incoherent ($\gamma \rightarrow \infty$, $\Delta \rightarrow \infty$, or $J \rightarrow 0$), at the incoherent limit $\sqrt{\mathcal{L} - 1}$ can be simplified as

$$\sqrt{\mathcal{L} - 1} \simeq \frac{x\sqrt{2}}{y} = \frac{\sqrt{2}(\sqrt{\Delta^2 + J^2\langle\theta_1^\dagger\theta_2\rangle^2} - \Delta)}{|J|\langle\theta_1^\dagger\theta_2\rangle}. \quad (\text{A2})$$

Omitting the Frank-Condon factor in denominator since the remaining terms can already approximate the coherent to incoherent behaviour of delocalization, we obtain

$$\sqrt{\mathcal{L} - 1} \simeq \frac{\sqrt{2}(\sqrt{\Delta^2 + J^2\langle\theta_1^\dagger\theta_2\rangle^2} - \Delta)}{|J|}. \quad (\text{A3})$$

Approximating the Frank-Condon factor with $e^{-\gamma}$, the above expression leads to Eq. (13).

¹R. E. Blankenship, *Molecular Mechanisms of Photosynthesis* (Wiley-Blackwell, Oxford, 2002).

²*Organic Photovoltaics: Concepts and Realization*, edited by C. Brabec, V. Dyakonov, J. Parisi, and N. Sariciftci (Springer, Berlin, 2003).

³Y.-C. Cheng and G. R. Fleming, *Annu. Rev. Phys. Chem.* **60**, 241 (2009).

⁴A. Ishizaki and G. R. Fleming, *J. Chem. Phys.* **130**, 234110 (2009).

⁵A. Olaya-Castro and G. D. Scholes, *Int. Rev. Phys. Chem.* **30**, 49 (2011).

⁶S. Jang and Y.-C. Cheng, *WIREs Comput. Mol. Sci.* **3**, 84 (2013).

⁷H. Wiesenhofer, D. Beljonne, G. D. Scholes, E. Hennebicq, J.-L. Bredas, and E. Zojer, *Adv. Funct. Mater.* **15**, 155 (2005).

⁸G. S. Engel, T. R. Calhoun, E. L. Read, T. K. Ahn, T. Mancal, Y.-C. Cheng, R. E. Blankenship, and G. R. Fleming, *Nature (London)* **446**, 782 (2007).

⁹E. Collini and G. D. Scholes, *Science* **323**, 369 (2009).

- ¹⁰E. Collini, C. Y. Wong, K. E. Wilk, P. M. G. Curmi, P. Brumer, and G. D. Scholes, *Nature (London)* **463**, 644 (2010).
- ¹¹G. Panitchayangkoon, D. Hayes, K. A. Fransted, J. R. Caram, E. Harel, J. Wen, R. E. Blankenship, and G. S. Engel, *Proc. Natl. Acad. Sci. U.S.A.* **107**, 12766 (2010).
- ¹²D. Beljonne, C. Curutchet, G. D. Scholes, and R. J. Silbey, *J. Phys. Chem. B* **113**, 6583 (2009).
- ¹³N. Makri and D. E. Makarov, *J. Chem. Phys.* **102**, 4600 (1995).
- ¹⁴N. Makri and D. E. Makarov, *J. Chem. Phys.* **102**, 4611 (1995).
- ¹⁵A. Ishizaki and G. R. Fleming, *J. Chem. Phys.* **130**, 234111 (2009).
- ¹⁶J. Prior, A. Chin, S. Huelga, and M. Plenio, *Phys. Rev. Lett.* **105**, 050404 (2010).
- ¹⁷P. Nalbach and M. Thorwart, *J. Chem. Phys.* **132**, 194111 (2010).
- ¹⁸P. Nalbach, A. Ishizaki, G. R. Fleming, and M. Thorwart, *New J. Phys.* **13**, 063040 (2011).
- ¹⁹C. Kreisbeck, T. Kramer, M. Rodriguez, and B. Hein, *J. Chem. Theory Comput.* **7**, 2166 (2011).
- ²⁰A. W. Chin, J. Prior, R. Rosenbach, F. Caycedo-Soler, S. F. Huelga, and M. B. Plenio, *Nat. Phys.* **9**, 113 (2013).
- ²¹S. Jang, Y.-C. Cheng, D. R. Reichman, and J. D. Eaves, *J. Chem. Phys.* **129**, 101104 (2008).
- ²²S. Jang, *J. Chem. Phys.* **131**, 164101 (2009).
- ²³S. Jang, *J. Chem. Phys.* **135**, 034105 (2011).
- ²⁴A. Nazir, *Phys. Rev. Lett.* **103**, 146404 (2009).
- ²⁵D. McCutcheon and A. Nazir, *Phys. Rev. B* **83**, 165101 (2011).
- ²⁶A. Kolli, A. Nazir, and A. Olaya-Castro, *J. Chem. Phys.* **135**, 154112 (2011).
- ²⁷R. J. Silbey and T. Harris, *J. Chem. Phys.* **80**, 2615 (1984).
- ²⁸D. P. S. McCutcheon and A. Nazir, *J. Chem. Phys.* **135**, 114501 (2011).
- ²⁹D. P. S. McCutcheon, N. S. Dattani, E. M. Gauger, B. W. Lovett, and A. Nazir, *Phys. Rev. B* **84**, 081305(R) (2011).
- ³⁰F. A. Pollock, D. P. S. McCutcheon, B. W. Lovett, E. M. Gauger, and A. Nazir, *New J. Phys.* **15**, 075018 (2013).
- ³¹M. Grover and R. J. Silbey, *J. Chem. Phys.* **54**, 4843 (1971).
- ³²R. Silbey and R. Munn, *J. Chem. Phys.* **72**, 2763 (1980).
- ³³H.-T. Chang and Y.-C. Cheng, *J. Chem. Phys.* **137**, 165103 (2012).
- ³⁴A. Kolli, E. J. O'Reilly, G. D. Scholes, and A. Olaya-Castro, *J. Chem. Phys.* **137**, 174109 (2012).
- ³⁵E. N. Zimanyi and R. J. Silbey, *Philos. Trans. R. Soc. London, Ser. A* **370**, 3620 (2012).
- ³⁶C. K. Lee, J. Moix, and J. Cao, *J. Chem. Phys.* **136**, 204120 (2012).
- ³⁷H. van Amerongen, L. Valkunas, and R. van Grondelle, *Photosynthetic Excitons* (World Scientific, Singapore, 2000).
- ³⁸E. Silinš and V. Čápek, *Organic Molecular Crystals: Interaction, Localization, and Transport Phenomena* (American Institute of Physics, New York, 1994).
- ³⁹T. Holstein, *Ann. Phys.* **8**, 343 (1959).
- ⁴⁰H. Dekker, *Phys. Rev. A* **35**, 1436 (1987).
- ⁴¹A. J. Leggett, S. Chakravarty, A. T. Dorsey, M. P. A. Fisher, A. Garg, and W. Zwerger, *Rev. Mod. Phys.* **59**, 1 (1987).
- ⁴²V. Kenkre and R. Knox, *Phys. Rev. B* **9**, 5279 (1974).
- ⁴³T.-C. Yen and Y.-C. Cheng, *Procedia Chem.* **3**, 211 (2011).
- ⁴⁴M. K. Grover and R. Silbey, *J. Chem. Phys.* **52**, 2099 (1970).
- ⁴⁵R. P. Feynman and F. L. Vernon, *Ann. Phys.* **24**, 118 (1963).
- ⁴⁶J. Eckel, S. Weiss, and M. Thorwart, *Eur. Phys. J. B* **53**, 91 (2006).
- ⁴⁷D. P. S. McCutcheon and A. Nazir, *New J. Phys.* **12**, 113042 (2010).
- ⁴⁸Y.-C. Cheng and R. J. Silbey, *J. Phys. Chem. B* **109**, 21399 (2005).
- ⁴⁹V. Kenkre, *Phys. Rev. B* **11**, 1741 (1975).
- ⁵⁰D. J. Thouless, *Phys. Rep.* **13**, 93 (1974).
- ⁵¹T. C. Berkelbach, D. R. Reichman, and T. E. Markland, *J. Chem. Phys.* **136**, 034113 (2012).